SYNCHROTRON X-RAY DIFFRACTION STUDY OF PINEAPPLE LEAF FIBER REINFORCED NATURAL RUBBER COMPOSITES DURING STRETCHING

Thapanee Wongpreedee[1] and Taweechai Amornsakchai[2, 3*]

Received: June 18, 2015; Revised date: September 22, 2015; Accepted date: September 22, 2015

Abstract

Structural development in preferentially aligned short pineapple leaf fiber (PALF) reinforced natural rubber (NR) composites was investigated with synchrotron wide angle X-ray scattering (WAXS) during stretching. NR and NR reinforced with 2 types of PALF, i.e. untreated and sodium hydroxide-treated PALF, were found to have different stress-strain behaviors. Normally, NR displays very low stress in the low strain region. This pattern changed considerably with the addition of the PALF. Stress for the composites increased sharply in the initial strain region and then remained roughly constant in the strain range of 60 to 200% before displaying an upturn. The composite containing sodium hydroxide-treated PALF displays a stress upturn at a lower strain than that with untreated PALF. A comparison of the WAXS patterns for stretched NR and the NR-PALF composites revealed that the onset of crystallization of the NR in the NR-PALF composites occurred at a lower macroscopic strain than that in the NR. Both types of NR-PALF composites display similar crystallinity at the same strain. Analysis of azimuthal scans of the 2 composites revealed a better orientation of the amorphous phase in the composite containing the sodium hydroxide-treated PALF. This suggests that the early stress upturn in the system containing treated PALF should be attributed to better stress transfer to the fiber.

Keywords: Natural rubber, pineapple leaf fiber, composite, WAXS, strain-induced crystallization

Introduction

Rubber is a soft polymeric material that can be deformed to a length many times its original length and has the ability to regain its original shape. Natural rubber (NR) stands out for its excellent mechanical properties owing to its ability to undergo strain-induced crystallization at very high strains. The mechanical properties of rubber can be altered by the addition of different types of fillers such as carbon black, silica, clay, synthetic and natural fibers, and

[1] *Program in Materials Science and Engineering, Faculty of Science, Mahidol University, Bangkok, 10400, Thailand.*

[2] *Department of Chemistry and Center of Excellence for Innovation in Chemistry, Faculty of Science, Mahidol University, Nakorn Pathom, 73170, Thailand.*

[3] *Center of Sustainable Energy and Green Materials, Faculty of Science, Mahidol University, Nakorn Pathom, 73170, Thailand. E-mail: taweechai.amo@mahidol.ac.th*

[*] *Corresponding author*

graphene (Blow and Hepburn, 1982; Donnet and Custodero, 2005; Lopattananon *et al*., 2006; Fukahori, 2008; Rezende *et al*., 2010; Eldho *et al*., 2012; Kengkhetkit and Amornsakchai, 2012; Prasertsri and Rattanasom, 2012). Generally, incorporation of these fillers increases the modulus of the rubber. The availability of synchrotron wide angle X-ray scattering (WAXS) has allowed in-situ investigation of the structural development in NR during stretching (Toki *et al*., 2002; Tosaka *et al*., 2004; Candau *et al*., 2012; Toki, 2014). It was found that the presence of certain fillers in NR caused the onset of strain-induced crystallization to occur at lower strains (Poompradub *et al*., 2005; Gonzalez *et al*., 2008a, 2008b; Ozbas *et al*., 2012). This has been attributed to the strain amplification effect of the added rigid filler. Despite the addition of the same filler content, the degree to which the strain is amplified may not be the same. This indicates that each type of filler imparts changes in the mechanical properties via different mechanisms. Fillers with a very high aspect ratio, such as nanoclay and functionalized graphene sheet, have been shown to promote much early onset of strain-induced crystallization.

In recent years, environmental-friendly products in various industries have attracted a great deal of interest. Natural fibers, such as banana fiber, pineapple leaf fiber (PALF), sisal fiber, and hemp fiber, are alternative fillers to synthetic fibers for the reinforcement of composites. PALF has attractive properties of high strength and modulus when compared with other natural fibers. The tensile strength and modulus of PALF are approximately 413-1,627 MPa and 34.5-82.5 GPa, respectively (Satyanarayana *et al*., 1982; Susheel *et al*., 2009).

In addition, PALF can be obtained from the pineapple leaf which is one of Thailand's agricultural wastes (Kengkhetkit and Amornsakchai, 2012). The main components of PALF include cellulose (67.0-82.0%), hemicellulose (9.5-18.8%), lignin (4.4-15.4%), pectin (1.2-3.0%), and waxes (3.2-4.2%) (Sapuan *et al*., 2011). We have studied PALF reinforced rubbers as well as NR. These fiber reinforced rubber composites display very distinct stress-strain behavior, i.e. a sharp rise in stress at relatively low strains. This characteristic is not obtainable from rubbers with particulate fillers or even with nanoclay, nanocellulose, or graphene. Such a very different behavior would naturally appeal for investigation of strain-induced crystallization in the matrix rubber.

In this work, WAXS was used to investigate the structural development in PALF-reinforced NR during stretching for a better understanding of the reinforcing mechanism. The knowledge and understanding on these effects would be important in developing better NR composites. Two types of PALF, i.e. as prepared or untreated PALF and sodium hydroxide-treated PALF were investigated. The PALF content was fixed at 10 parts (by weight) per hundred of rubber (phr), since a greater PALF content would cause a severe drop in elongation at the break of the composite (Lopattananon *et al*., 2006; Kalapakdee and Amornsakchai, 2014 Wisittanawat *et al*., 2014a).

Materials and methods

Materials and Methods

Natural rubber (NR) grade STR 5L was purchased from Natcha Chemicals Co., Ltd., Bangkok, Thailand. All rubber chemicals and sodium hydroxide were commercial grade.

Pineapple leaf was supplied from Kok Kwai District, Amphor Ban Rai, Uthai Thani Province, Thailand. The pineapple leaf was chopped into 6 mm lengths and milled with a small disc milling machine, as previously reported (Kengkhetkit and Amornsakchai, 2012).

Pineapple Leaf Fiber (PALF) Treatment

The PALF was immersed in 10% w/v of NaOH solution for 30 min. The PALF was then filtered out, washed with tap water several times, and dried in a hot air oven. The untreated PALF is coded as UPALF and that treated with sodium hydroxide as TPALF. The UPALF has an average diameter of 18.70 μm while the TPALF has an average diameter of 11.47 μm. The aspect ratios

of the UPALF and TPALF are approximately 320 ± 48 and 523 ± 55, respectively. The UPALF has lignin, hemicellulose, and cellulose contents of 0.1, 18.5, and 73.1%, respectively, and those contents of the TPALF are 0.1, 5.6, and 90.8%, respectively. Figure 1 displays the scanning electron micrograph of the UPALF and TPALF. The images were taken with a Hitachi scanning electron microscope (S2500, Hitachi Ltd., Tokyo, Japan).

Preparation of NR/PALF Composites

The formulations of the NR and NR/PALF composites are shown in Table 1. The amount of the PALF was fixed at 10 phr. The composite compounds were coded as NR/10UPALF and NR/10TPALF for the untreated and treated PALF, respectively. The compounds were mixed in a laboratory 2-roll mill to produce mixtures with fibers aligned in the machine direction, as described previously (Wisittanawat *et al*.,

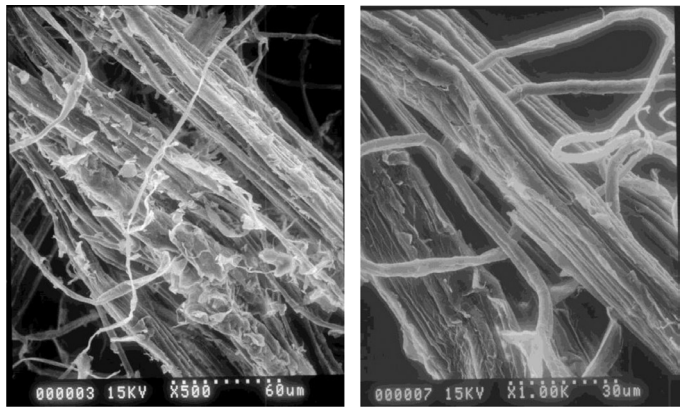

Figure 1. SEM images of UPALF (left) and TPALF (right)

Table 1. Formulation of NR and NR/PALF composites

Ingredient	NR	NR/10UPALF	NR/10TPALF
NR STR5L	100	100	100
PALF	-	10	-
TPALF	-	-	10
ZnO	5	5	5
Steric acid	2	2	2
CBS	1	1	1
Sulphur	2	2	2

Table 2. Mixing steps of NR and NR/PALF composites

Step		NR	NR/PALF composites
1	Rubber mastication	8 min (0-8 min)	2 min (0-2 min)
2	Slowly add PALF	-	6 min (2-8 min)
3	ZnO + Steric acid	3 min (8-11 min)	3 min (8-11 min)
4	CBS	2 min (11-13 min)	2 min (11-13 min)
5	Sulphur	2 min (13-15 min)	2 min (13-15 min)

2014a; Kalapakdee and Amornsakchai, 2014). The sequence of ingredient addition is shown in Table 2. Each composite was vulcanized at 150°C for cure times obtained from tests on a moving die rheometer.

Mechanical Test

The tensile behavior of the samples was investigated by using an Instron Universal Test Instrument (model 5566, Instron, Norwood, MA, USA). The test was conducted according to ISO 37 (International Organization for Standardization, 2011). The sample was dumb-bell-shaped according to Die C, ISO 37. The gauge length was 25 mm and the crosshead speed was 500 mm/min. Strain was determined with a long travel contact-style extensometer.

WAXS Studies

WAXS was performed at Beamline BL1.3W at the Synchrotron Light Research Institute (Public Organization), Thailand. The X-ray energy was 9.5 keV. The plane of the rubber sheet and the fiber direction were perpendicular to the beam direction. The samples were stretched to different levels of nominal strains (0%, 50%, 100%, 200%, 400%, 500%, and 600%) and the WAXS patterns were recorded with a Mar detector. The 2-theta scan on the equator line was averaged over the azimuthal angle of 5° on both sides of the equator. Data were analyzed with the Saxsit program, a self-developed program for small angle X-ray scattering (Rugmai and Soontaranon, 2015).

The crystallinity, X_c, of each sample was calculated from the intensity data of its equatorial 2-theta scan using Equation 1.

$$X_c = \left(\frac{A_c}{(A_c + A_a)} \right) \times 100 \quad (1)$$

when A_c = Areas of crystalline region
A_a = Areas of amorphous region

Results and discussion

Mechanical Properties

The stress-strain curves of NR and the NR/PALF composites (NR/10UPALF and NR/10TPALF) in the longitudinal and transverse directions are shown in Figure 2. The large difference between the stress-strain curves in the 2 directions confirms the preferential alignment of the PALF. With an increasing strain, the stress of NR increases gradually and then increases sharply at the high strain region before breaking. On the other hand, the stress of the NR/PALF composite increases sharply in the initial strain region and then remains stable in the strain range of 60 to 200%. Afterwards, the stress

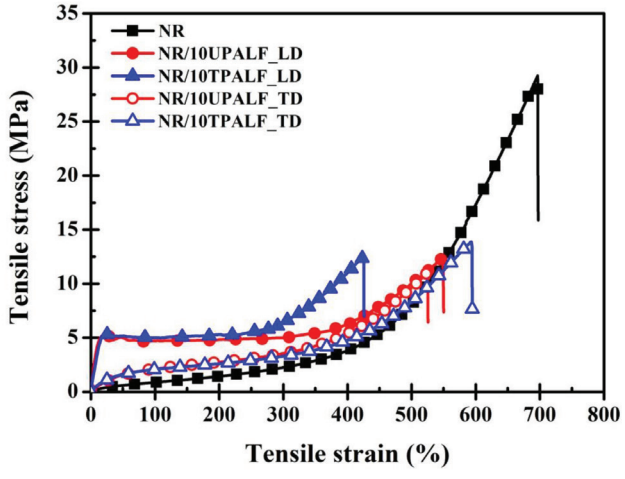

Figure 2. Stress-strain curves of NR and NR/PALF composites

increases sharply at the high strain region. The tensile stress of the NR/PALF samples in the low strain region is much higher than that of NR. In addition, the stress-strain curve of the NR/10UPALF displays an upturn in stress at a slightly lower strain than that of NR. That of the NR/10TPALF displays such an upturn even at the lower strain. The strains at which a deflection in the stress is observed for NR, NR/10UPALF, and NR/10TPALF are 400, 350, and 250%, respectively. Although the stress-strain curves of the NR/10UPALF and NR/10TPALF resemble the cold-drawing behavior of semi-crystalline polymers, the mechanism is different. It should be noted that both the NR/10UPALF and NR/10TPALF do not return to their original lengths once deformed beyond the yield-like point which designates fiber debonding (Wisittanawat *et al*., 2014b). The stresses at which the composites break are quite similar and lower than that of NR. This is because failure at such a large extension is determined by the presence of defects (Setua and De, 1985; Akhtar *et al*., 1986; Wisittanawat *et al*., 2014b).

The upturn or deflection in stress is generally attributed to strain-induced crystallization of NR. It is thus straightforward to ask if such a shift of the stress upturn relates to the shift of the onset of strain-induced crystallization. To answer the question, structural studies using WAXS would be required.

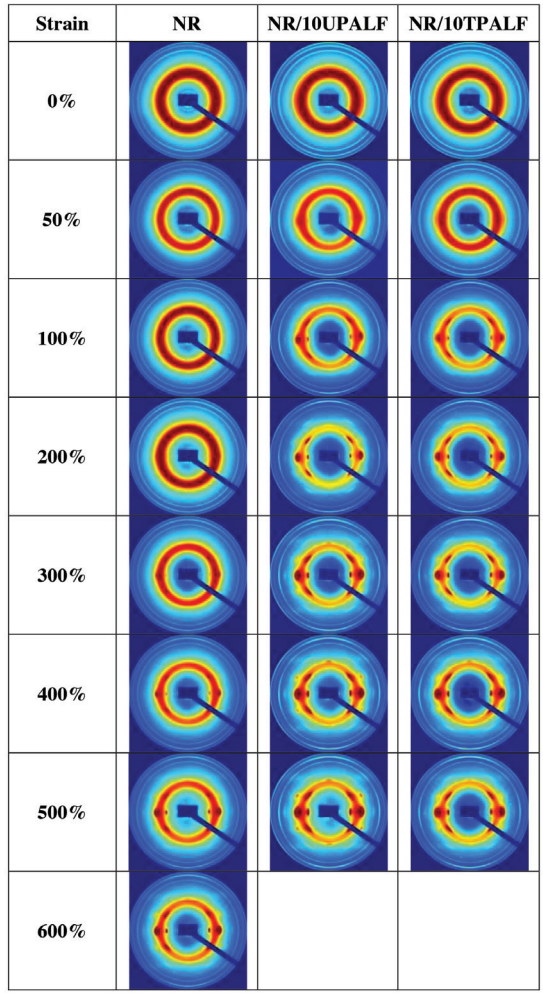

Figure 3. WAXS patterns of NR, NR/10UPALF, and NR/10TPALF composites stretched to different strains

WAXS of NR and NR/PALF Composites During Stretching

To study the effect of the PALF on the reinforcement of NR, the structure of NR and NR/PALF were investigated using WAXS.

Figure 3 shows the WAXS patterns of NR and NR/PALF stretched to different nominal strains. All un-stretched samples display a halo pattern indicating the amorphous nature of the material. When the samples were stretched to higher strains, the crystalline reflection peaks indexed as the 200,120, and 201 reflections appear, albeit at different strain levels NR seems to exhibit the strain-induced crystallization at a strain around 200% while for NR in the composite containing PALF, the strain-induced crystallization starts to appear at a strain of approximately 50%.

In order to see clearly the emergence of crystalline reflections in the stretched samples,

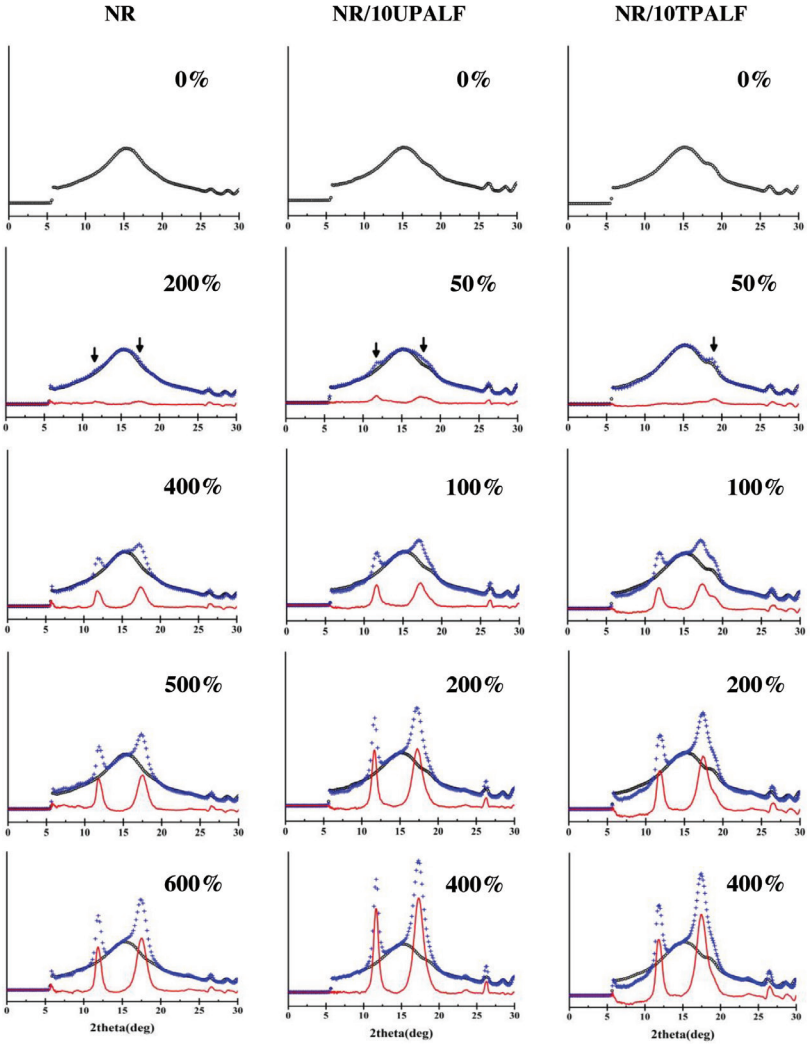

Figure 4. Equatorial 2-theta scans (+) (averaged over +/- 5 degree from the equator) of NR, NR/10UPALF, and NR/10TPALF composites stretched to different strains. For each strain, the amorphous background (◡) is substracted from the corresponding 2-theta scan to yield the crystalline signal (—). The down arrows indicate the onset of strain-induced crystallization

a 2-theta scan on the equator will be considered. Figure 4 shows the equatorial 2-theta scan from 5° to 30° of the WAXS patterns of NR and the 2 NR/PALF composites stretched to different strains. The intensities of 200 and 120 reflections of each sample increase with increasing the strain. For each scan, the corresponding amorphous background was subtracted to obtain only the crystalline peaks. These data are then used to calculate the crystallinity for the stretched samples using Equation 1 and the results are shown in Figure 5.

From Figure 5, the crystallinity of NR/10UPALF and NR/10TPALF increases with the increasing strain. That for NR/10UPALF appears to increase linearly and reaches approximately 24% while that for NR/10TPALF starts to level off at approximately 19%. The crystallinity of NR remains close to 0 up to a strain of approximately 300% and then increases with roughly a similar rate to that of NR/10UPALF. However, the crystallinity of NR appears to reach a plateau of about 16%. It should be noted that the crystallinity here may not be directly comparable to that reported elsewhere (Toki *et al*., 2003). It can, however, be used to illustrate the structural development within this work.

It appears that the presence of the PALF indeed affects the onset of strain-induced crystallization. A similar phenomenon has been observed in nanoclay-filled NR (Gonzalez *et al*., 2008a) and functionalized graphene sheet-filled NR (Ozbas *et al*. 2012). However, the onset of strain-induced crystallization of NR may not always relate to the upturn in the stress observed in the tensile experiment.

The early onset of strain-induced crystallization in nanoclay-filled NR (Gonzalez *et al*., 2008a) and functionalized graphene sheet-filled NR (Ozbas *et al*., 2012) has been attributed to different mechanisms. The former was attributed to the formation of a completely aligned physical network of nanoclay and this is suggested to favor the alignment of NR chains and thus increase the crystallization rate (Gonzalez *et al*., 2008a). The latter was, however, attributed to the increase in surface area which in turn increased the amount of immobilized NR chains. The greater amount of immobilized rubber renders a very high strain amplification (Ozbas *et al*., 2012). Since our PALF has much less surface area than graphene and it contains no functional group of immobilized NR chains, the mechanism for the promotion of an early strain-induced crystallization should be different from that with nanoplates. It is generally accepted that the stress transfer in short fiber reinforced composite occurs via a shearing mechanism between the fiber and the matrix (Cox, 1952; Hull and Clyne, 1996). The matrix has, according to the theory, zero shear strain at the middle of the fiber and the shear strain progressively increases towards both ends of the fiber. Since the fiber is many times stiffer than the matrix rubber and, thus, would not deform, there would be an extremely high

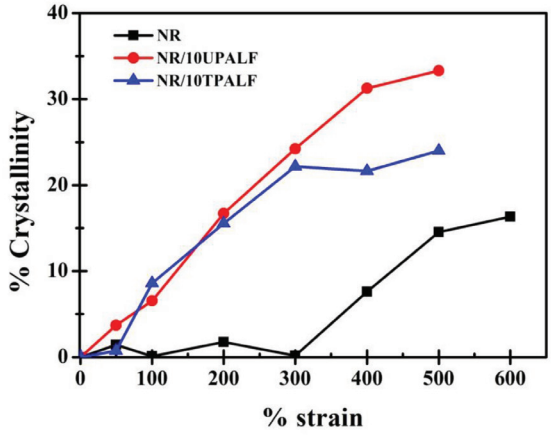

Figure 5. Crystallinity of NR and NR/PALF composites stretched to different strains

shear strain at the fiber-matrix interface to accommodate the much greater macroscopic strain. It is believed that the NR chains that stay on, or close to, the fiber surface would be highly strained and crystallize first. Although there is only 10 phr of PALF and the fraction of NR in contact with the fiber may not be considered high enough to contribute to the observed change in macroscopic behavior, it should be noted that the shearing mechanism is not confined only to the interface but could extend far beyond. The level of shear strain would progressively decrease as the distance from the interface increases.

Still there are some differences between the effect of the UPALF and TPALF on the macroscopic stress-strain behavior of the composites. NR/10TPALF displays a stress upturn at a lower strain that does NR/10UPALF. The 2, however, display virtually the same crystallinity. To find out if there are other differences in the matrix microstructure, azimuthal scans at 2-theta of 14.25-14.50 degrees, which is the peak of the amorphous ring, were carried out and the results are shown in Figure 6. An azimuthal scan contains both amorphous and crystalline signals. The 2 crystalline signals at about -39 and 39 degrees are the shoulders of the (201) reflection. The change in intensity of the amorphous over the azimuthal angle provides information on the amorphous orientation (Murakami *et al*., 2002; Ikeda *et al*., 2007; Amnuaypornsri *et al*., 2012). It is seen that the amorphous orientations in NR and NR/10UPALF stretched to 200, 300, and 400% strains are relatively low. This is in agreement with what has been reported by other groups (Murakami *et al*., 2002; Amnuaypornsri *et al*., 2012; Ikeda *et al*., 2007). There is, however, a clear signal for amorphous orientation in NR/10TPALF. The relative amount of amorphous orientation with respect to that randomly aligned can be determined by the method used by Murakami *et al*. (2002) with slight modification. Here the ratio of the intensities at the azimuthal angle of 0 degree to 90 degrees is used. The values for NR, NR/10UPALF, and NR/10TPALF are displayed in Table 3. It can be seen that the amorphous orientation at a fixed strain becomes greater with the addition of the PALF and that TPALF gives the greatest value. The amorphous orientation for each material

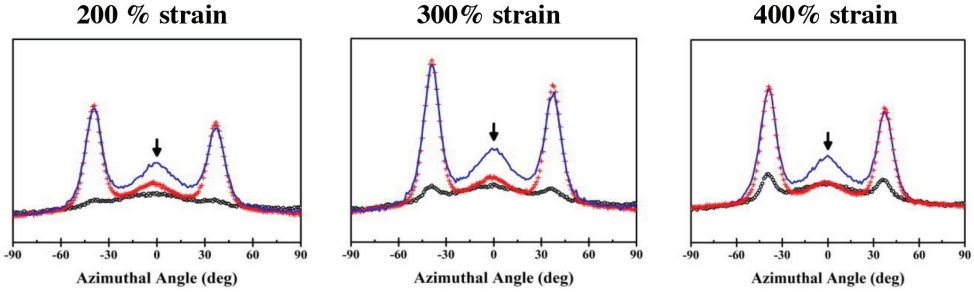

Figure 6. Azimuthal scans at 2-theta = 14.25-14.50 degrees for NR(○), NR/10UNPALF, (+) and NR/10TPALF (—) composites stretched to selected strains. The down arrows indicate the position for amorphous orientation

Table 3. Ratios of the intensities at the azimutal angle of 0 degree to 90 degrees (Iequator/Imeridian) for NR and NR/PALF composites stretched to different strains

Strain	200%	300%	400%
NR	1.23	1.25	1.26
NR/10UPALF	1.34	1.37	1.26
NR/10TPALF	1.54	1.64	1.51

increases with the increasing strain. However, the amorphous orientations for NR/10UPALF and NR/10TPALF decrease at 400% strain. This probably indicates the occurrence of stress relaxation at very high strains.

From the results shown above, the presence of the PALF in NR causes the NR to crystallize at a much lower macroscopic strain than it normally does. The PALF also promotes greater crystallinity (Figure 5). Furthermore, the sodium hydroxide-treated PALF causes additional friction of the NR chains to orient along the stretching direction. It is difficult to completely visualize what is happening during the entire stretching process. More work is definitely needed before complete understanding could be gained. It may, however, be worthwhile to ttempt to explain these observations. Since it is widely accepted that no load is transferred directly through the fiber ends, it would follow that the oriented NR chains in NR/PALF composites are chains that are stretched via the shearing mechanism. Sodium hydroxide treated PALF presumably has a smoother surface and thus provides better and more intimate contact with the matrix rubber. Such a better contact would then give better frictional stress transfer and more NR chains would be stretched as a result. Additional contact areas are also created as a result of the finer diameter of the TPALF. Thus, the number of stretched chains should be greater than that in the case of the UPALF. It is postulated that among these stretched chains, some chains remain non-crystalline, as observed in the azimuthal scans. These stretched non-crystalline chains may be groups of parallel chains that do not have a regular lateral order or long range order. It is these groups of chains that cause the early stress upturn during the stretching of the NR/10TPALF composite. A contribution also comes from the development in crystallinity which is similar for both the NR/10UPALF and NR/10TPALF composites.

Conclusions

The presence of the PALF in the NR matrix has caused a considerable change in the macroscopic stress-strain behavior of the material. The tensile stress in the low strain region for the NR/PALF composite is much greater than that of the NR. In addition, the surface treatment of the fiber affects the stress-strain behavior further. Synchrotron's WAXS studies have revealed that the presence of the fiber also affects the onset of the strain-induced crystallization of the matrix rubber, indicating a region with very high local molecular strain at a relatively very low macroscopic strain. The presence of the fiber also increases the maximum crystallinity of NR. The nature of the surface of the fiber does not, however, affect the maximum crystallinity of NR but increases the amorphous orientation.

Acknowledgement

Partial financial support from the Center for Innovation in Chemistry: Postgraduate Education and Research Program in Chemistry (PERCH-CIC), Commission on Higher Education, Ministry of Education is gratefully acknowledged.

References

Akhtar, S., Bhowmick, A.K., De, P.P., and De, S.K. (1986). Tensile rupture of short fiber filled thermoplastic elastomer. J. Mater. Sci., 21:4179-4184.

Amnuaypornsri, S., Toki, S., Hsiao, B.S., and Sakdapipanich, J. (2012). The effects of endlinking network and entanglement to stress-strain relation and strain-induced crystallization of un-vulcanized and vulcanized natural rubber. Polymer, 53:3325-3330.

Blow, C.M. and Hepburn, C. (1982). Rubber Technology and Manufacture. 2nd ed. Butterworths, London, UK, 608p.

Candau, N., Chazeau, L., Chenal, J.M., Gauthier, C., Ferreira, J., Munch, E., and Rochas, C. (2012). Characteristic time of strain induced crystallization of crosslinked natural rubber. Polymer, 53(13): 2540-2543.

Cox, H.L. (1952). The elasticity and strength of paper and other fibrous materials. Brit. J. Appl. Phys., 3:72–79.

Donnet, J.B. and Custodero, E. (2005). Reinforcement of elastomers by particulate fillers. In: Science and Technology of Rubber. 3rd ed. Mark, J.E., Erman, B., and Eirich, F.R., (eds). Elsevier Academic Press, San Diego, CA, USA, p. 367-400.

Eldho, A., Elbi, A.P., Deepa, B., Jyotishkumar, P., Pothen, A.L., Narine, S.S., and Thomas, S. (2012). X-ray diffraction and biodegradation analysis of green composites of natural rubber/nanocellulose. Polym. Degrad. Stabil., 97(10):2378-2387.

Fukahori, Y. (2008). Mechanism of the carbon black reinforcement of rubbers. In: Current Topics in Elastomers Research. Bhowmick, A.K., (ed). CRC Press, Boca Raton, FL, USA, p. 518.

Gonzalez, J.C., Retsos, H., Verdejo, R., Toki, S., Hsiao, B.S., Giannelis, E.P., and Lopez-Manchado, M.A. (2008a). Effect of nanoclay on natural rubber microstructure. Macromolecules, 41(18): 6763-6772.

Gonzalez, J.C., Verdejo, R., Toki, S., Hsiao, B.S., Giannelis, E.P., and Lopez-Manchado, M.A. (2008b). Real-time crystallization of organoclay nanoparticle filled natural rubber under stretching. Macromolecules, 41(7):2295-2298.

Hull, D. and Clyne, T.W. (1996). An Introduction to Composite Materials. 2nd ed. Cambridge University Press, New York, NY, USA, 326p.

Ikeda, Y., Yasuda, Y., Makino, S., Yamamoto, S., Tosaka, M., Senoo, K., and Kohjiya, S. (2007). Strain-induced crystallization of peroxide-crosslinked natural rubber. Polymer, 48:1171-1175.

International Organization for Standardization. (2011). ISO 37: Rubber, vulcanized or thermoplastic – Determination of tensile stress-strain properties. International Organization for Standardization, Geneva, Switzerland.

Kengkhetkit, N. and Amornsakchai, T. (2012). Utilisation of pineapple leaf waste for plastic reinforcement: 1. A novel extraction method for short pineapple leaf fiber. Ind. Crop. Prod., 40:55-61.

Kalapakdee, A. and Amornsakchai, T. (2014). Mechanical properties of preferentially aligned short pineapple leaf fiber reinforced thermoplastic elastomer: Effects of fiber content and matrix orientation. Polym. Test., 37:36-44.

Lopattananon, N., Panawarangkul, K., Sahakaro, K., and Ellis, B. (2006). Performance of pineapple leaf fiber-natural rubber composites: The effect of fiber surface treatments. J. Appl. Polym. Sci., 102(2): 1974-1984.

Murakami, S., Senoo, K., Toki, S., and Kohjiya, S. (2002). Structural development of natural rubber during uniaxial stretching by in situ wide angle X-ray diffraction using a synchrotron radiation. Polymer, 43(7):2117-2120.

Ozbas, B., Toki, S., Hsiao, B.S., Chu, B., Register, A.R., Aksay, A.I., Prud'homme, K.R., and Adamson, H.D. (2012). Strain-induced crystallization and mechanical properties of functionalized graphene sheet-filled natural rubber. J. Polym. Sci. Polym. Phys., 50(10):718-723.

Prasertsri, S. and Rattanasom, N. (2012) Fumed and precipitated silica reinforced natural rubber composites prepared from latex system: Mechanical and dynamic properties. Polym. Test., 31(5):593-605.

Poompradub, S., Tosaka, M., Kohjiya, S., Ikeda, Y., Toki, S., Sics, I., and Hsiao, B.S. (2005). Mechanism of strain-induced crystallization in filled and unfilled natural rubber vulcanizates. J. Appl. Phys., 97(10):103529.

Rezende, C.A., Bragança, F.C., Doi, T.R., Lee, L-T., Galembeck, F., and Boué, F. (2010). Natural rubber-clay nanocomposites: Mechanical and structural properties. Polymer, 51(16):33644-3652.

Rugmai, S. and Soontaranon, S.. (2015). Small Angle X-ray Scattering Image Tool. Nakhon Ratchasima, Thailand: Synchrotron Light Research Institute. Available from: www.slri.or.th/th/beamlines/SAXS. Accessed date: Mar 20, 2015.

Setua, D.K. and De, S.K. (1985). Effect of short fibers on critical cut length in tensile failure of rubber vulcanizates. J. Mater. Sci., 20:2653-2660.

Susheel, K., Kaith, B.S., and Inderjeet, K., (2009). Pretreatments of natural fibers and their application as reinforcing material in polymer composites - a review. Polym. Eng. Sci., 49(7): 1253-1272.

Sapuan, S.M., Mohamed, A.R., Siregar, J.P., and Ishak, M.R. (2011). Pineapple leaf fibers and PALF-reinforced polymer composite. In: Cellulose Fibers: Bio-and Nano-polymer Composites: Green Chemistry and Technology. Susheel, K., Kaith, B.S., and Kaur, I. (eds). Springer, New York, NY, USA, p. 325-344.

Satyanarayana, K.G., Pillai, C.K.S., Pillai, S.G.K., and Sukumaran, K., (1982). Structure property studies of fibers from various parts of the coconut tree. J. Mater.Sci. 17:2453-2462.

Toki, S. (2014). The effect of strain-induced crystallization (SIC) on the physical properties of natural rubber (NR). In: Chemistry, Manufacture and Applications of Natural Rubber. Shinzo, K. and Yuko, I. (eds). Elsevier, London, UK, p. 135-167.

Tosaka, M., Murakami, S., Poompradub, S., Kohjiya, S., Ikeda, Y., Toki, S., Sics, I., and Hsiao, B.S. (2004). Orientation and crystallization of natural rubber network as revealed by WAXD using synchrotron radiation. Macromolecules, 37(9):3299-3309.

Toki, S., Sics, I., Ran, S., Liu, L., and Hsiao, B.S. (2002). New insights into structural development in natural rubber during uniaxial deformation by in situ synchrotron X-ray diffraction. Macromolecules, 35(17):6578-6584.

Toki, S., Sics, I., Ran, S., Liu, L., and Hsiao, B.S. (2003). Molecular orientation and structural development in vulcanized polyisoprene rubbers during uniaxial deformation by in situ synchrotron X-ray diffraction. Polymer, 44:6003-6011.

Wisittanawat, U., Thanawan, S., and Amornsakchai,

T. (2014a). Mechanical properties of highly aligned short pineapple leaf fiber reinforced - nitrile ubber composite: effect of fiber content and bonding agent. Polym. Test., 35:20-27.

Wisittanawat, U., Thanawan, S., and Amornsakchai, T. (2014b). Remarkable improvement of failure strain of preferentially aligned short pineapple leaf fiber reinforced nitrile rubber composites with silica hybridization. Polym. Test., 38:91-99.